Original Article

PMP

Progress in Medical Physics 32(4), December 2021
https://doi.org/10.14316/pmp.2021.32.4.137
eISSN 2508-4453

Development of a Beam Source Modeling Approach to Calculate Head Scatter Factors for a 6 MV Unflattened Photon Beam

So-Yeon Park, Noorie Choi, Na Young Jang

Department of Radiation Oncology, Veterans Health Service Medical Center, Seoul, Korea

Received 30 November 2021
Revised 9 December 2021
Accepted 14 December 2021

Corresponding author
Na Young Jang
(mumuki79@gmail.com)
Tel: 82-2-2225-4647
Fax: 82-2-2225-4640

Purpose: This study aimed to investigate the accuracy of head scatter factor (S_c) by applying a developed multi-leaf collimator (MLC) scatter source model for an unflattened photon beam.
Methods: Sets of S_c values were measured for various jaw-defined square and rectangular fields and MLC-defined square fields for developing dual-source model (DSM) and MLC scatter model. A 6 MV unflattened photon beam has been used. Measurements were performed using a 0.125 cm^3 cylindrical ionization chamber and a mini phantom. Then, the parameters of both models have been optimized, and S_c has been calculated. The DSM and MLC scatter models have been verified by comparing the calculated values to the three S_c set measurement values of the jaw-defined field and the two S_c set measurement values of MLC-defined fields used in the existing modeling, respectively.
Results: For jaw-defined fields, the calculated S_c using the DSM was consistent with the measured S_c value. This demonstrates that the DSM was properly optimized and modeled for the measured values. For the MLC-defined fields, the accuracy between the calculated and measured S_c values with the addition of the MLC scatter source appeared to be high, but the only use of the DSM resulted in a significantly bigger differences.
Conclusions: Both the DSM and MLC models could also be applied to an unflattened beam. When considering scattered radiation from the MLC by adding an MLC scatter source model, it showed a higher degree of agreement with the actual measured S_c value than when using only DSM in the same way as in previous studies.

Keywords: Head scatter factor, Unflattened photon beam, Multi-leaf collimator, Dual-source model

Introduction

With the development of radiation therapy technology, intensity-modulated radiation therapy (IMRT) and volumetric modulated radiation therapy (VMAT) are being widely used in various cancer treatments [1-4]. They can modulate fluence maps by using the multi-leaf collimator (MLC) to deliver high-dose radiation to treatment targets while delivering minimal dose of radiation to surrounding normal organs [5]. To deliver optimized dose distribution to patients, fluence complexity must be improved, and many MLC movements are required for its implementation. As such, the MLC is a critical factor in radiation therapy.

The head scatter factor (S_c) is the relative ratio of all scattered radiation amounts from the head of the linear accelerator (linac). According to the American Association of Physicists in Medicine (AAPM) Task Group (TG)-74 report, the main causes of scattered radiation include the primary

collimator, flattening filter, jaw, and MLCs [6]. The AAPM TG-74 report has mentioned that scattered radiation by the MLC is no longer negligible as IMRT and VMAT use several small and irregular MLC fields [6]. This led to the increased importance of scattered radiation from the MLC, and research was needed accordingly. Nevertheless, previous studies have developed models that did not consider scattered radiation from MLCs; these models were dual- and three-source models in which S_c is calculated by measuring the area of the model using detector's eye view (DEV) [7-9]. When the MLC is located in a specific area as shown in Fig. 1a, it is exposed to the radiation field and creates scattered radiation; however, it is not considered in DEV; thus, it does not affect the S_c calculation. Only when the MLCs enter the DEV area (Fig. 1b), it can affect the S_c calculation. The MLC cannot be considered as present in region "a" of Fig. 1c (the region where the MLC-defined square field size is from 8×8 to 15×15 cm^2 after the jaw-defined field size is fixed to 15×15 cm^2); thus, the S_c value in the field where the scattered radiation from MLCs is not considered is calculated similarly, resulting in a difference in the measured S_c value. In the "b" region (the region where the MLC-defined square field size is 4×4 to 8×8 cm^2 after the jaw-defined field size is fixed to 15×15 cm^2), the position of the MLC affects the DEV; thus, the calculated S_c value decreases as the field size decreases. In terms of area "a," it is a very small difference between the calculated and measured S_c values, but in the case of IMRT or VMAT, which use hundreds of segments and control points, the combined difference can be large. Previously, we have developed an additional model that can consider scattered radiation from the MLCs [10]. A model for considering scattered radiation from MLCs was located at the MLC location in the linac. The model was developed including line and area sources with scatter interface which was used for determining affected and unaffected areas. Details for scatter interface have been mentioned in the previous study [10]. This model has been verified using a 6 MV photon beam. The results showed that the model was more accurate than the existing model, and particularly, the accuracy increased for very small and irregular fields. For this developed model, the accuracy of the independent verification program could be improved, and a more accurate pretreatment quality management evaluation was enabled.

The unflattened filter (FFF) photon beam is a photon beam from which the flattened filter has been removed in the linac. For small fields, it has radiation quality and profiles similar to those of the flattened filter (FF) but has the advantage of rapidly ending the radiation treatment when dose rates increase by 2–4 times. As the demand for stereotactic ablative radiotherapy (SABR) increased, the use of unflattened filter photon beams also increased. The MLC models developed in the previous studies have not yet been verified for unflattened filter photon beams. When one of the most important factors of scattered radiation, the

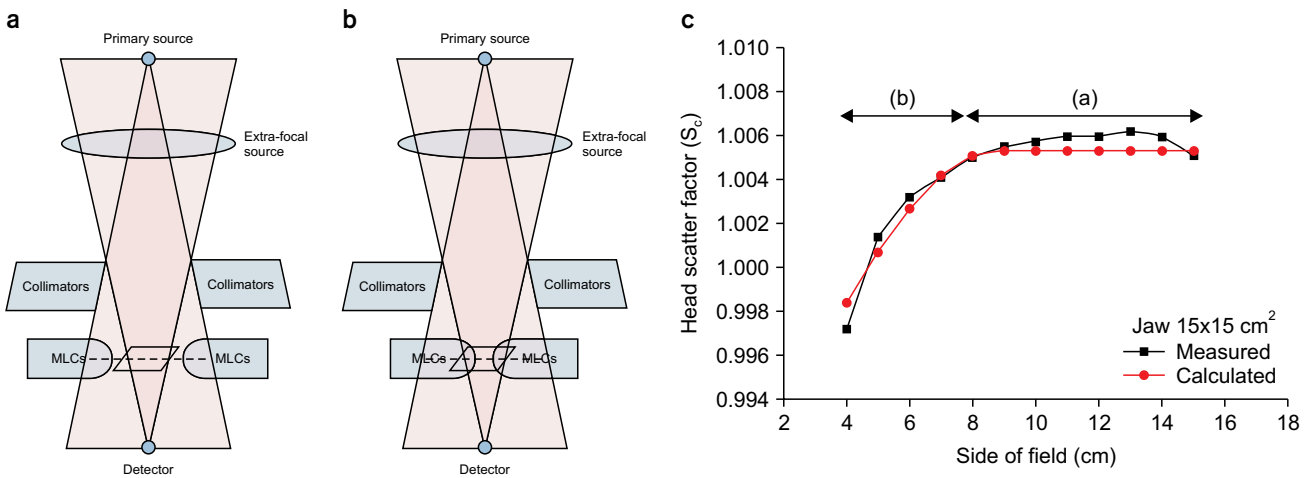

Fig. 1. Schematics of the geometrical relationship between the jaws and multi-leaf collimators (MLCs) in terms of the beam's eye view, detector's eye view, and scatter interface for (a) unaffected area, (b) affected area, and (c) head scatter factor (S_c) as a function of the MLC-defined square field size ranging from 4×4 to 15×15 cm^2 at a fixed jaw setting of 15×15 cm^2. The calculated S_c values are derived from the dual-source model.

flattening filter, is removed, it is expected to have a significant influence on the model. Therefore, this study aims to verify the developed model for the unflattened filter photon beam.

Materials and Methods

1. Measurement for head scatter factors

Various S_c sets were measured for the development of the dual-source model (DSM) and the MLC scatter model. A 6 MV unflattened photon beam from a Varian Clinac® TrueBeam STx linear accelerator that is equipped with 60 pairs of millennium MLCs (Varian Medical Systems, Palo Alto, CA, USA) has been used. Measurements have been performed using a 0.125 cm^3 cylindrical ionization chamber (Model 31010; PTW Freiburg, Freiburg, Germany) and a mini phantom (Model 670; CIRS Inc., Norfolk, VA, USA). The source-to-chamber distance was 100 cm, and the depth was 10 cm.

For the development of the DSM, the S_c of various jaw-defined square and rectangular fields has been measured. Here, all MLCs were in a retracted state. For the development of the MLC scatter model, the jaw was fixed, and then the S_c of various MLC-defined square fields was measured. The field setup for this measurement is illustrated in Table 1. To reduce the uncertainty in S_c measurement, the measurement was repeated at least 5 times, and the standard deviation was within 0.3%. The reference field was a jaw-defined size of 10×10 cm^2.

2. Development of source models

The DSM proposed by Jiang et al. [11], as explained in previous studies, is a model that considers all the scattered radiation from the head of the linac and the backscattered radiation reentering the monitor chamber, with an extrafocal source located at the location of the existing FF. S_c is obtained by measuring the area radiated from the DEV to the extrafocal source. As mentioned earlier, for all scattered radiation from the head, the scattered radiation from the MLC was not considered [10,11]. It was subjected to a process of optimizing the DSM parameters using the S_c values for various jaw-defined fields. The jaw-defined fields used during this process include a total of 3 sets, 4×4 to 40×40 cm^2 square fields alongside the rectangular field, i.e., 10×4 to 10×40 cm^2 and 4×10 to 40×10 cm^2 with both the X and Y jaws fixed at 10 cm.

In this study, the DSM parameters were iteratively optimized using the trust-region-reflective algorithm for nonlinear least squares (MathWorks, Inc., Natick, MA, USA) to match the calculated S_c with the measured one for the jaw-defined square and rectangular fields (Table 1). The objective function was the chi-square difference between the measured and calculated S_c values for the jaw-defined fields with the fully retracted MLCs. Optimization was performed within the maximum number of iterations (400) until the objective function reached below a termination tolerance

Table 1. Measurement cases for modeling and evaluating the dual-source and MLC scatter source

	Jaw-defined field (X×Y cm^2)	MLC-defined field (X×Y cm^2)
Dual-source model		
For development	4×4 to 40×40	Open (MLC retracted)
	10×4 to 10×40	
	4×10 to 40×10	
For evaluation	4×4 to 4×40	
	4×4 to 40×4	
	40×4 to 40×40	
	4×40 to 40×40	
MLC scatter source model		
For development	10×10	4×4 to 10×10
	20×20	4×4 to 20×20
For evaluation	15×15	4×4 to 15×15

MLC, multi-leaf collimator.

(10^{-6}) [10].

The MLC scatter model developed in previous studies consists of line and area source, that is, scattered radiation from the end of the MLC tip and scattered radiation from the MLC area, respectively [10]. If the jaw-defined field is fixed and the MLC-defined field increases, the scattered radiation from the tip of the MLC increases, but the scattered radiation from the MLC area decreases. By formulating each of these, $S_{c,MLC}$ can be defined as follows:

$$S_{c,MLC}=S_{c,line}\cdot S_{c,area} \quad (1)$$

The calculated $S_{c,MLC}$ can be used to obtain the S_c for an MLC-defined field. The fields used for modeling included a set of S_c values obtained when the MLC-defined field is 4×4 to 10×10 cm^2 with a jaw fixed at 10×10 cm^2 and a set of S_c values obtained when the MLC-defined field is 4×4 to 20×20 cm^2 with a jaw fixed at 20×20 cm^2, i.e., a total of two sets. Details are available in previous studies [10].

Similarly, the parameters were optimized using the same optimization methods as in DSM to attain the best fit between the measured and calculated $S_{c,MLC}$ values.

3. Evaluation of source models

For the verification of the DSM, the calculated S_c values were compared to the three S_c set measurement values of the jaw-defined fields used in the existing modeling. For further verification, the calculated values were also compared with the S_c set measurement values that were not

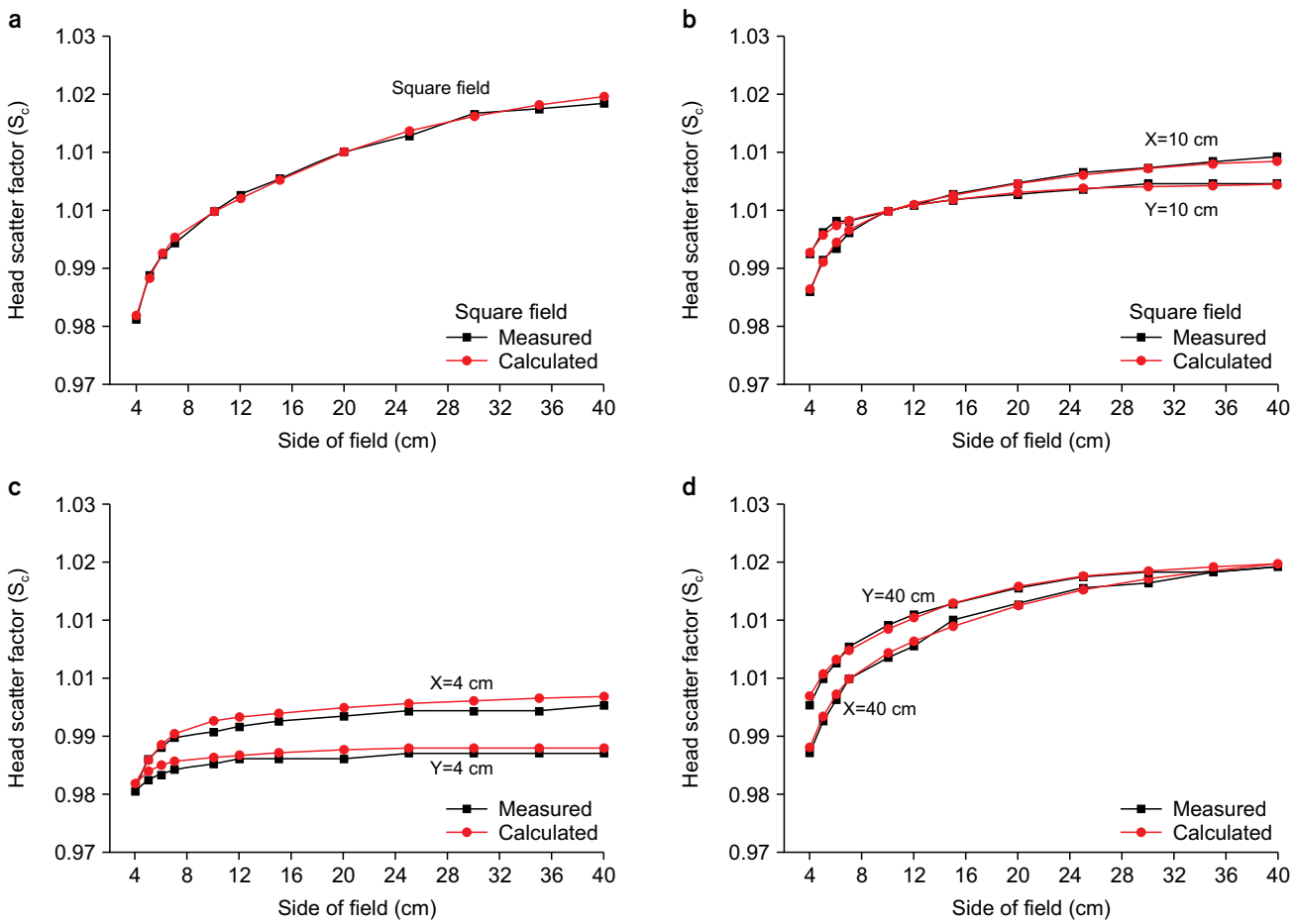

Fig. 2. Comparison between the calculated and measured head scatter factor (S_c) values for (a) square fields ranging from 4×4 to 40×40 cm^2; (b) rectangular fields with one pair of jaws fixed at 10 cm, while the other pair varied from 4 to 40 cm; (c) rectangular fields with one pair of jaws fixed at 4 cm while the other pair varied from 4 to 40 cm; and (d) rectangular fields with one pair of jaws fixed at 40 cm, while the other pair varied from 4 to 40 cm. The calculated S_c values are derived from the dual-source model.

used in the existing modeling. These are S_c measurement values for a total of 4 sets of 4×4 to 4×40 cm^2 and 4×4 to 40×4 cm^2 with X and Y jaws fixed at 4 cm along with 40×4 to 40×40 cm^2 and 4×40 to 40×40 cm^2 with X and Y jaws fixed at 40 cm, respectively, which are the rectangular fields.

To verify the MLC scatter source model, two S_c set measurement values of MLC-defined fields used in the existing modeling and calculated values have been compared. For further verification, the calculated values have also been compared to the S_c set measurement values that were not used in the existing modeling. This is a set of S_c values when an MLC-defined field is 4×4 to 15×15 cm^2 in a state where the jaw is fixed at 15×15 cm^2. The equation for evaluating the accuracy using percent error is as follows:

$$Percent\ error\ (\%)=\frac{S_c\,(mea)-S_c\,(cal)}{S_c\,(cal)}\times 100 \qquad (2)$$

Results

1. Evaluation of jaw-defined square fields

In this study, the DSM has been evaluated using jaw-defined square fields ranging from 4×4 to 40×40 cm^2 and rectangular fields with one pair of jaws fixed at 4, 10, or 40 cm while the other pair varied from 4 to 40 cm. Fig. 2 shows the S_c values calculated by DSM and measured S_c values for the jaw-defined field size. Table 2 quantifies and shows the difference between the measured S_c value and the calculated S_c value for each measurement set. Overall, S_c calculated using the DSM and the measured S_c showed a good agreement. It can be identified that all difference values are within 0.212%. This suggests that the DSM has been properly optimized and modeled for the measured values.

2. Evaluation of multi-leaf collimator-defined square fields

The optimization parameters for the MLC scatter source

Table 2. Differences between the measured and calculated S_c values for jaw-defined field sizes

Field	Jaw-defined field size (X×Y cm^2)	Mean (%)	Maximum (%)
Square field	4×4 to 40×40	0.050	0.114
Rectangular field	10×4 to 10×40	0.036	0.099
	4×10 to 40×10	0.025	0.075
	4×4 to 4×40	0.130	0.212
	4×4 to 40×4	0.116	0.164
	40×4 to 40×40	0.065	0.112
	4×40 to 40×40	0.055	0.154

S_c, head scatter factor.

Table 3. Optimal parameter values of the multi-leaf collimator scatter source for an unflattened 6 MV beam

Parameter	Jaw-defined field size (X×Y cm^2)		
	10×10	20×20	30×30
$ES_{mlc,out}$			
a_{out}	0.010	0.011	0.012
b_{out}	0.642	0.621	0.598
σ_{out}	14.125	36.835	303.745
$ES_{mlc,in}$			
a_{in}	0.012	0.008	0.005
b_{in}	0.552	0.491	0.477
σ_{in}	26.402	38.458	385.015

ES, extrafocal source.

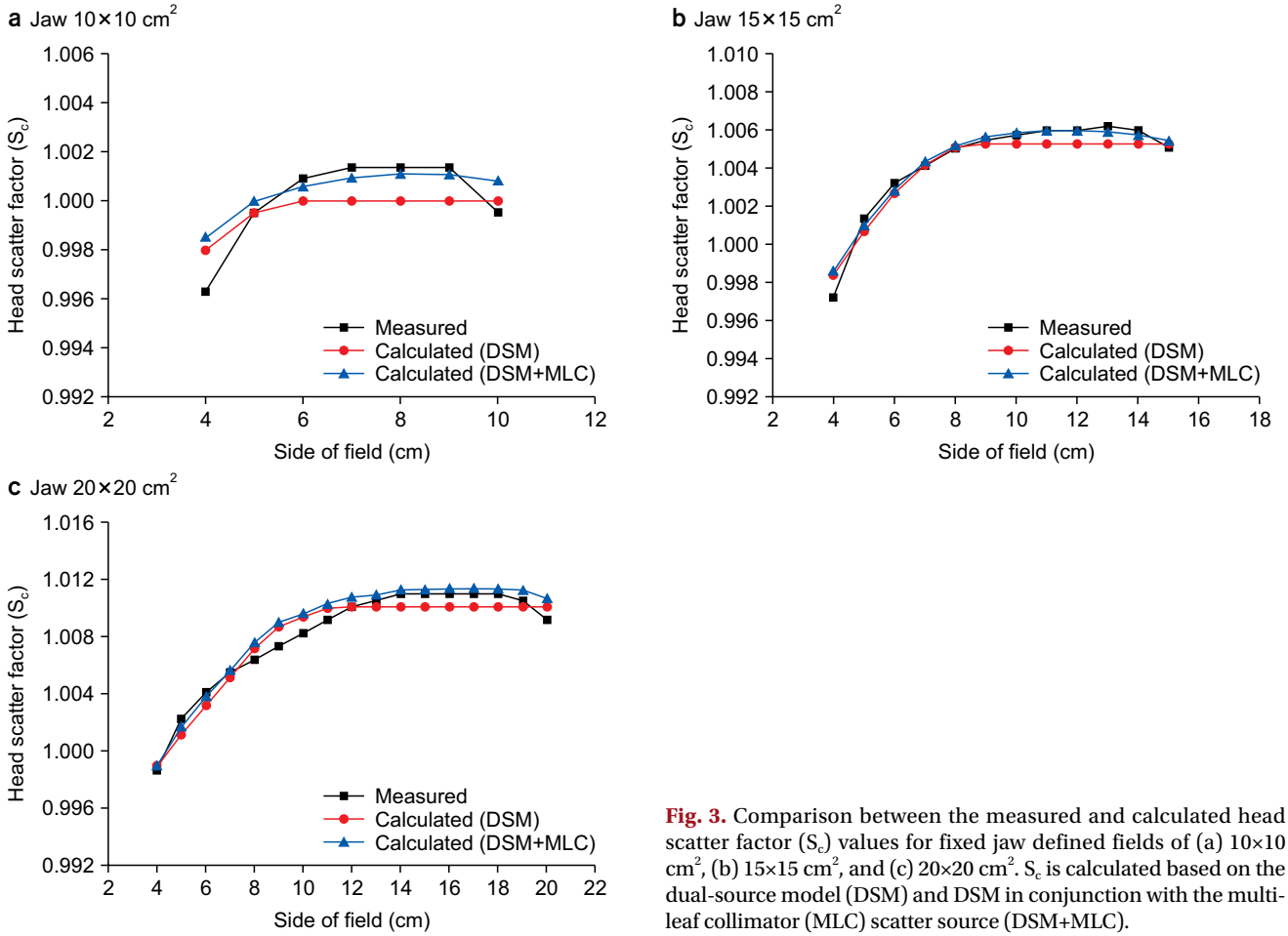

Fig. 3. Comparison between the measured and calculated head scatter factor (S_c) values for fixed jaw defined fields of (a) 10×10 cm^2, (b) 15×15 cm^2, and (c) 20×20 cm^2. S_c is calculated based on the dual-source model (DSM) and DSM in conjunction with the multi-leaf collimator (MLC) scatter source (DSM+MLC).

Table 4. Differences between the measured and calculated S_c values for MLC-defined square field sizes ranging from 4×4 cm^2 to the fixed jaw opening size

Jaw-defined field size (cm^2)	DSM[a]		DSM+MLC[b] (this work)		*P*-value
	Mean (%)	Maximum (%)	Mean (%)	Maximum (%)	
10×10	0.109	0.169	0.090	0.217	0.051
15×15	0.095	0.116	0.055	0.136	< 0.001
20×20	0.114	0.133	0.056	0.163	< 0.001

S_c, head scatter factor; MLC, multi-leaf collimator; DSM, dual-source model.
[a]Developed by Jiang et al. [11].
[b]DSM in conjunction with MLC scatter source developed in this study.

model have been determined using nonlinear least squares. Table 3 demonstrates the optimization parameters for line and area source of MLC scatter sources. There was no clear trend for each parameter. These optimization parameters were used to model the MLC scatter source, the calculated S_c values were compared with the measured S_c values, and S_c values were calculated using only DSM (Fig. 3). For all jaw-defined fields, if the MLC-defined field size becomes greater than or equal to the specific MLC-defined field size, the S_c value calculated using the DSM remained flat, which causes a difference from the measured S_c value. In the case of the calculated S_c value with the addition of the MLC scatter source, its accuracy with the measured S_c value appeared to be high. Table 4 demonstrates the quantified degree of accuracy. Overall, a small difference has been observed between the calculated value and the measured val-

ue, but the additional use of the MLC scatter source model resulted in a significantly smaller difference in probability. Particularly, if the jaw-defined field was 15×15 cm^2, a difference of 0.055% has been observed when an additional MLC scatter source was used.

Discussion

Previous studies have developed sources that are capable of modeling scattered radiation from the MLCs for flattened photon beams and have evaluated their performance [10]. When only DSM was used, the jaw-defined field area showed a high accuracy with the measured value, but when the MLC-defined field was used, it showed a low accuracy. When considering the scattered radiation from the MLCs by adding the MLC scatter source model developed in the previous study, the accuracy was higher than the S_c calculated using the DSM. However, previous studies have considered only the flattened photon beam, while this study has evaluated the performance when an unflattened photon beam was applied to the same MLC scatter source model.

Since the unflattened photon beam does not pass through FF, the S_c value is relatively less than that of the flattened beam [12,13]. Other studies have also examined these characteristics. However, the characteristic or tendency of S_c depending on the field size or depending on X or Y is the same as in the flattened beam [12,13]. Therefore, the DSM and MLC models could also be applied to the unflattened beam. The optimization parameter values for the MLC model are smaller than the optimization parameters obtained in previous research, which indicates that the amount of scattered radiation decreased compared with the flattened beam, resulting in a decrease in the associated weight value.

This study has several limitations. Measurements for small field sizes (less than 3×3 cm^2) could not be performed, which are mainly used in SABR. The difficulty in applying the modeling can be attributed to the physical limitation of the detector size and high measurement uncertainty for small fields [14,15]. It is assumed that more accurate modeling is possible if a small field size S_c is measured using a detector optimized for small fields, such as a diamond detector. Moreover, the amount of scattered radiation varies for high photon energy, and this should be considered. In a future study, we plan to apply scattered radiation modeling from the MLCs for high photon energy and evaluate its performance. Furthermore, since this study is empirical, Monte Carlo simulations are required to more accurately model scattered radiation from the MLC. Fig. 3c demonstrates that between MLC-defined field sizes of 8×8 and 12×12 cm^2, the S_c values calculated using the two models (DSM and DSM + MLC) are overestimated compared to the measured values. This suggests that scattered radiation from the MLC cannot be accurately divided using DEV. A more accurate MLC scatter source can be developed if scattered radiation from the MLC obtained in various MLC-defined field regions has been analyzed using a simulation.

Conclusions

This study aimed to evaluate the accuracy of S_c calculation by applying the previously developed MLC scatter source model to an unflattened photon beam. When considering scattered radiation from the MLCs by adding an MLC scatter source model, it showed a higher degree of agreement with the actual measured S_c value than when using only DSM in the same way as in previous studies. This MLC scatter source model is expected to be applied to the independent verification program in the future to enable more accurate dose calculation.

Acknowledgements

This study was supported by a VHS Medical Center Research Grant, Republic of Korea (grant number: VHSMC 21021).

Conflicts of Interest

The authors have nothing to disclose.

Availability of Data and Materials

All relevant data are within the paper and its Supporting Information files.

Author Contributions

Conceptualization: So-Yeon Park. Data curation: So-Yeon Park and Noorie Choi. Formal analysis: So-Yeon Park and Na Young Jang. Funding acquisition: Na Young Jang. Investigation: So-Yeon Park and Noorie Choi. Methodology: So-Yeon Park and Na Young Jang. Project administration: So-Yeon Park and Noorie Choi. Resources: So-Yeon Park. Software: So-Yeon Park and Na Young Jang. Supervision: Na Young Jang. Validation: So-Yeon Park and Noorie Choi. Visualization: So-Yeon Park and Na Young Jang. Writing–original draft: So-Yeon Park. Writing–review & editing: So-Yeon Park and Na Young Jang.

References

1. Ezzell GA, Galvin JM, Low D, Palta JR, Rosen I, Sharpe MB, et al. Guidance document on delivery, treatment planning, and clinical implementation of IMRT: report of the IMRT Subcommittee of the AAPM Radiation Therapy Committee. Med Phys. 2003;30:2089-2115.
2. Zhang P, Happersett L, Hunt M, Jackson A, Zelefsky M, Mageras G. Volumetric modulated arc therapy: planning and evaluation for prostate cancer cases. Int J Radiat Oncol Biol Phys. 2010;76:1456-1462.
3. Evans JD, Hansen CC, Tollefson MK, Hallemeier CL. Stereotactic body radiation therapy for medically inoperable, clinically localized, urothelial carcinoma of the renal pelvis: a case report. Adv Radiat Oncol. 2017;3:57-61.
4. Zhu X, Li F, Liu W, Shi D, Ju X, Cao Y, et al. Stereotactic body radiation therapy plus induction or adjuvant chemotherapy for early stage but medically inoperable pancreatic cancer: a propensity score-matched analysis of a prospectively collected database. Cancer Manag Res. 2018;10:1295-1304.
5. Park SY, Kim JI, Hoon Oh D, Park JM. Evaluation of the plan delivery accuracy of intensity-modulated radiation therapy by texture analysis using fluence maps. Phys Med. 2019;59:64-74.
6. Zhu TC, Ahnesjö A, Lam KL, Li XA, Ma CM, Palta JR, et al. Report of AAPM Therapy Physics Committee Task Group 74: in-air output ratio, Sc, for megavoltage photon beams. Med Phys. 2009;36:5261-5291.
7. Lam KL, Muthuswamy MS, Ten Haken RK. Flattening-filter-based empirical methods to parametrize the head scatter factor. Med Phys. 1996;23:343-352.
8. Kim S, Zhu TC, Palta JR. An equivalent square field formula for determining head scatter factors of rectangular fields. Med Phys. 1997;24:1770-1774.
9. Kim S, Palta JR, Zhu TC. The equivalent square concept for the head scatter factor based on scatter from flattening filter. Phys Med Biol. 1998;43:1593-1604.
10. Park SY, Kim S, Sung W, Kim ST. Modeling scattered radiation from multi-leaf collimators (MLCs) to improve calculation accuracy of in-air output ratio. Australas Phys Eng Sci Med. 2019;42:719-731.
11. Jiang SB, Boyer AL, Ma CM. Modeling the extrafocal radiation and monitor chamber backscatter for photon beam dose calculation. Med Phys. 2001;28:55-66.
12. Cho W, Kielar KN, Mok E, Xing L, Park JH, Jung WG, et al. Multisource modeling of flattening filter free (FFF) beam and the optimization of model parameters. Med Phys. 2011;38:1931-1942.
13. Xiao Y, Kry SF, Popple R, Yorke E, Papanikolaou N, Stathakis S, et al. Flattening filter-free accelerators: a report from the AAPM Therapy Emerging Technology Assessment Work Group. J Appl Clin Med Phys. 2015;16:5219.
14. Bagheri H, Soleimani A, Gharehaghaji N, Mesbahi A, Manouchehri F, Shekarchi B, et al. An overview on small-field dosimetry in photon beam radiotherapy: developments and challenges. J Cancer Res Ther. 2017;13:175-185.
15. Ghita M, McMahon SJ, Thompson HF, McGarry CK, King R, Osman SOS, et al. Small field dosimetry for the small animal radiotherapy research platform (SARRP). Radiat Oncol. 2017;12:204.